Biophysics and Physiological Modeling

Incorporating Molecular Biophysics in the Undergraduate Curriculum

Peter Hugo Nelson
Fisk University
circle4.com/biophysics
Moving beyond listening in BMB education Spotlight Session
ASBMB @ EB2021, 3:45 pm – 4:00 pm, April 30, 2021

Outline

- Introduction – Excel skills – the marble game
- Algorithmic thinking – kinetic Monte Carlo simulation
- Modeling change – finite difference (FD) methods (any differential model)
- Model validation – curve fitting and data analysis
- Thermodynamics for life sciences (and biochemistry)
  - osmosis and osmotic pressure – the chemical potential of water
  - ligand binding and enzyme kinetics
- Ion channels and membrane voltage
  - the Nernst potential
  - cell membrane is a capacitor
  - batteries and equivalent RC circuits
  - the action potential
- COVID-19 and epidemiology

Figures from
Biophysics and Physiological Modeling
ASBMB @ EB2021, April 30, 2021

Ch.1 Introduction – marble game

Figure 1.3 Photo of the marble game. It has ten marbles that can jump between two boxes. A ten-sided die is used to pick which marble jumps next.

Note: Chapters 1, 2, 3, 5 and 12 are available for free at http://circle4.com/biophysics/chapters/. There are also instructional videos and instructor guides. Visit http://circle4.com/biophysics/

- GlowScript Brownian motion simulation of the Marble Game

Instructions for using Excel start with the basics

	A	B	C
1	Turn	r	N_1
2	0		3
3	=A2+1		
4			
5			

	A	B	C
1	Turn	r	N_1
2	0		3
3	1		
4			
5			

Figure 1.7 Screenshots from Excel 2016, before and after hitting ENTER (see text).

- Implementing the Marble Game in a spreadsheet

Ch.2 Algorithms and pain relief

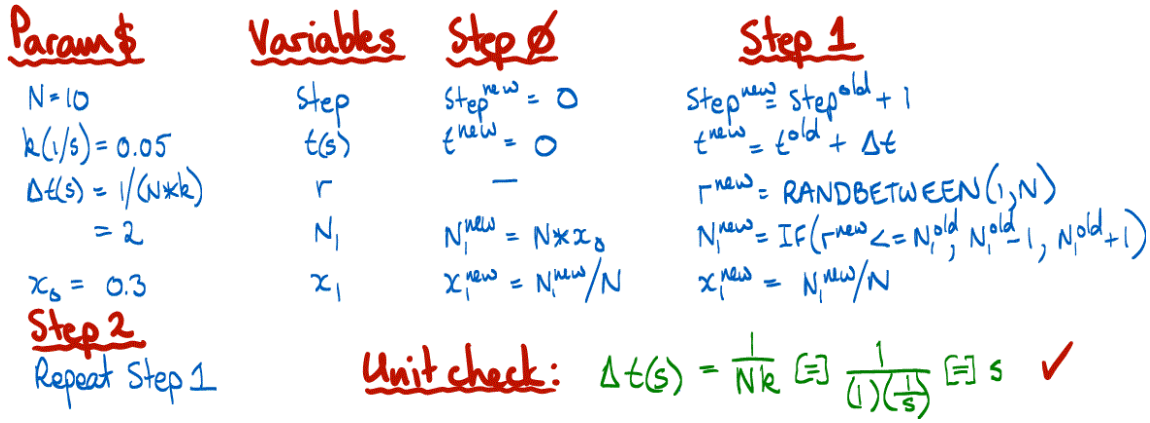

Figure 2.2 Algorithm for the marble game kMC sim shown in Figure 2.1.

Ch.3 Finite difference method and O_2

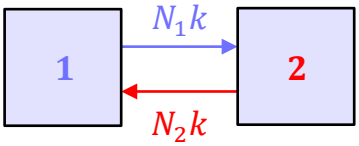

Fig.3.2 Finite difference (FD) diagram of the two-box marble game.

Finite difference equations

$$\delta N_1 = -N_1 k \delta t + N_2 k \delta t \tag{3.1}$$

By doing some algebra, equation (3.1) can be rearranged to give

$$\delta N_1 = (N_2 - N_1) k \delta t \tag{3.2}$$

Equation (3.2) is a **finite difference equation** (**FD equation**) that tells us how much N_1 changes (on average) during a short but **finite** amount of time δt.

- Comparing the FD method with the Marble Game kMC in a spreadsheet

Ch.5 A new model of osmosis

Hypothesis: Osmosis is the diffusion of water across a semipermeable barrier

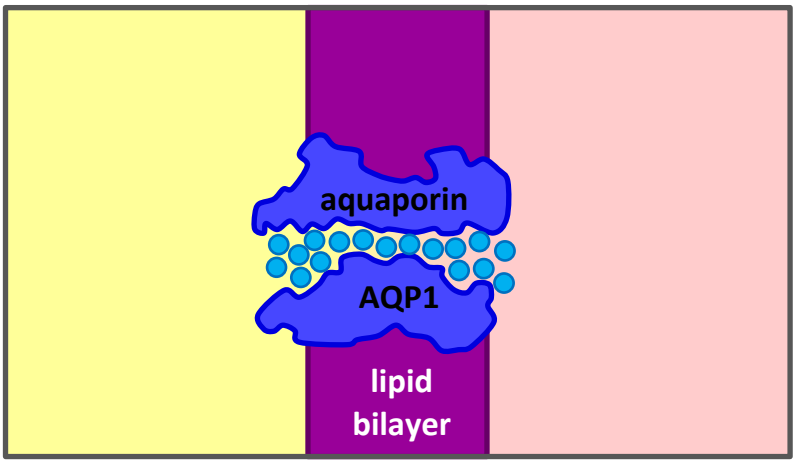

Fig.5.2 Schematic diagram of an AQP1 aquaporin protein (water channel) imbedded in a lipid bilayer membrane separating two solutions with differing effective water concentrations (after Murata *et al.* [2000]). The aquaporin provides a single-file pathway (shown in cross-section) for water molecules (circles) that makes the membrane semipermeable because only water molecules can pass through.

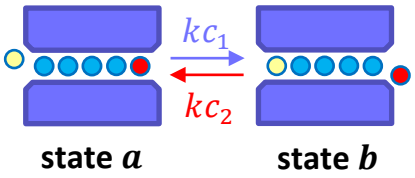

Fig.5.3 Schematic diagram of an AQP1 aquaporin selectivity filter showing the **knock-on jump** summary of single-file water permeation. The diagram shows two states (a and b) of the *same* AQP1 aquaporin. For the jump from state $a \rightarrow b$, the water molecule entering from box 1 is highlighted in yellow (lighter) and the water molecule knocked-on into box 2 is highlighted in red (darker). In the reverse $b \rightarrow a$ jump, the red water molecule enters from box 2 and the yellow water molecule is knocked-on into box 1.

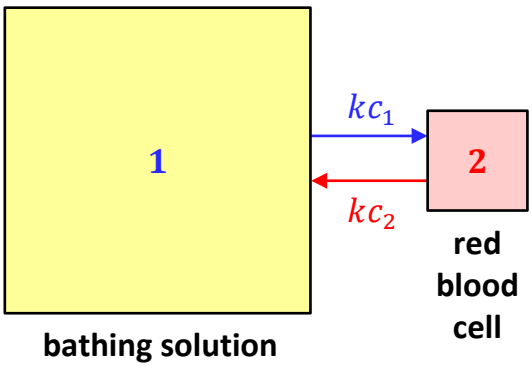

Fig.5.4 FD diagram of a red blood cell (box 2) floating in a large bathing solution (box 1). The water in the red blood cell has an effective concentration c_2 and the bathing solution has a constant effective water concentration c_1.

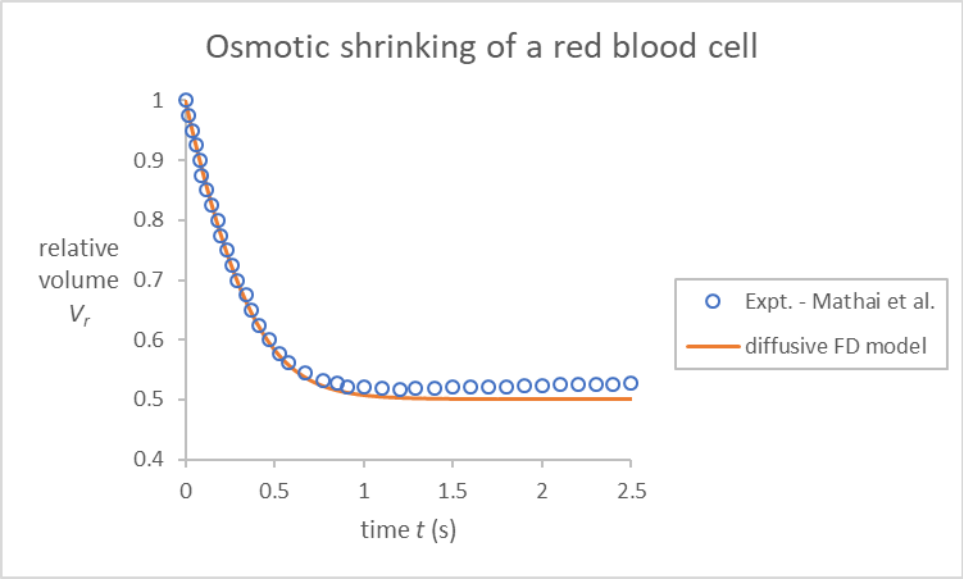

Fig.5.7 Excel chart showing the control (+/+) data from Fig. 5*A*. of Mathai *et al.* [1996] for the osmotic shrinking of a red blood cell, together with the diffusive model of osmosis calculated using FD equation (5.14). The experimental data were obtained by digitizing Fig. 5*A* and are reproduced here with permission from Mathai *et al.* [1996]).

Accounting for energy differences

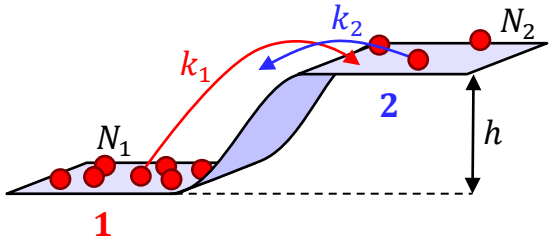

Fig.5.8 Schematic representation of the gravity marble game. The jump rate constant in the uphill direction (from box 1 → 2) is k_1. k_2 is the jump rate constant in the downhill direction (from box 2 → 1). The marbles each have mass m and the two boxes are separated by height h.

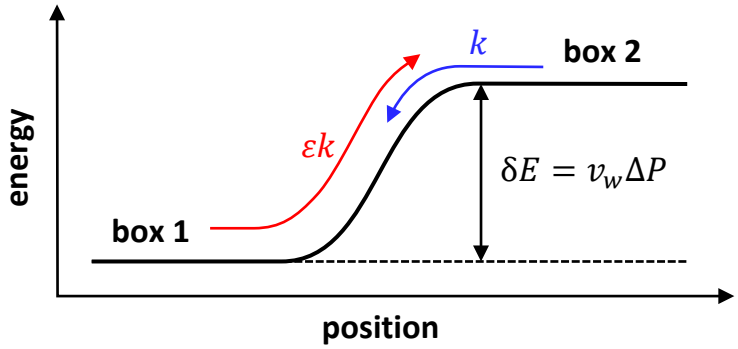

Fig.5.14 Simplified schematic energy diagram of osmosis with a (hydrostatic) pressure difference ΔP. The diagram shows a situation where box 2 has a higher pressure P_2 than box 1 with the difference given by $\Delta P = P_2 - P_1$. The water molecules each have volume v_w and the pressure difference ΔP raises the marble's potential energy by $\delta E = v_w \Delta P$ when it moves from box 1 → 2. The uphill jump rate is reduced by a factor $\varepsilon = 1 - \delta\psi$, where the small dimensionless energy step is $\delta\psi = \delta E/(k_B T)$.

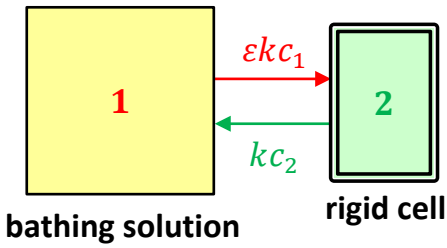

Fig.5.15 FD diagram of a rigid plant cell (box 2) in contact with a large bathing solution (box 1) within the **Helmholtz ensemble** (constant T, V). The water in the rigid plant cell has an effective water concentration c_2 and the bathing solution has a constant effective water concentration c_1. There is also a hydrostatic pressure difference $\Delta P = P_2 - P_1$ between the boxes that is maintained by the rigid cell wall of the plant cell. ΔP determines the value of the energy factor ε (5.44).

The new **diffusive model of osmosis** predicts the **van't Hoff equation**

$$\Delta\pi = \Delta s RT = -\Delta c RT \tag{5.68}$$

where $\Delta c = c_2 - c_1$ is the **effective water concentration difference** and $\Delta s = s_2 - s_1 = -\Delta c$ is the **osmolarity difference**.

Ch.6 Ligand binding and least-squares fits

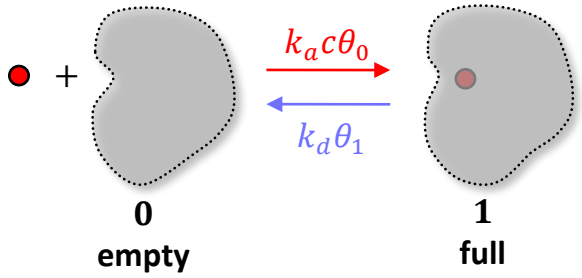

Fig.6.1 Schematic FD diagram of the single-occupancy binding model for an O_2 molecule (red circle) binding to a myoglobin molecule.

Students *show that* the ensemble average **occupancy** θ_1 of the myoglobin molecule is

$$\theta_1 = \frac{c}{K_d + c} \tag{6.4}$$

Students *test* the predictions of equation (6.4) by performing a **least-squares fit** in Excel using

$$Q = \sum_i r_i^2 \tag{6.11}$$

- Least squares fits in Excel using Solver

Sucrase enzyme kinetics

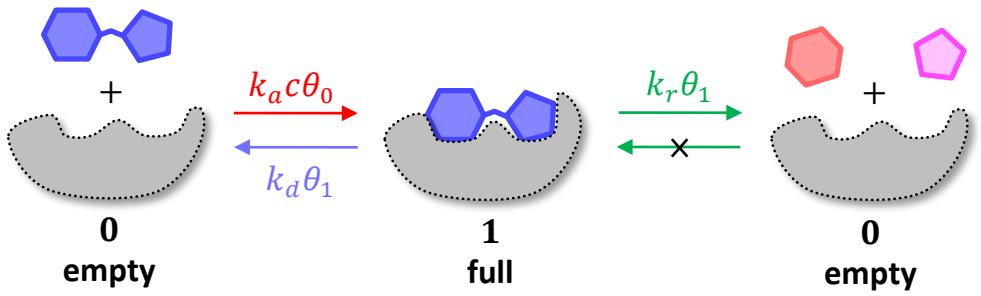

Fig.6.5 Schematic diagram of a sucrase enzyme hydrolyzing sucrose into glucose and fructose.

About what you discovered: Enzymes saturate

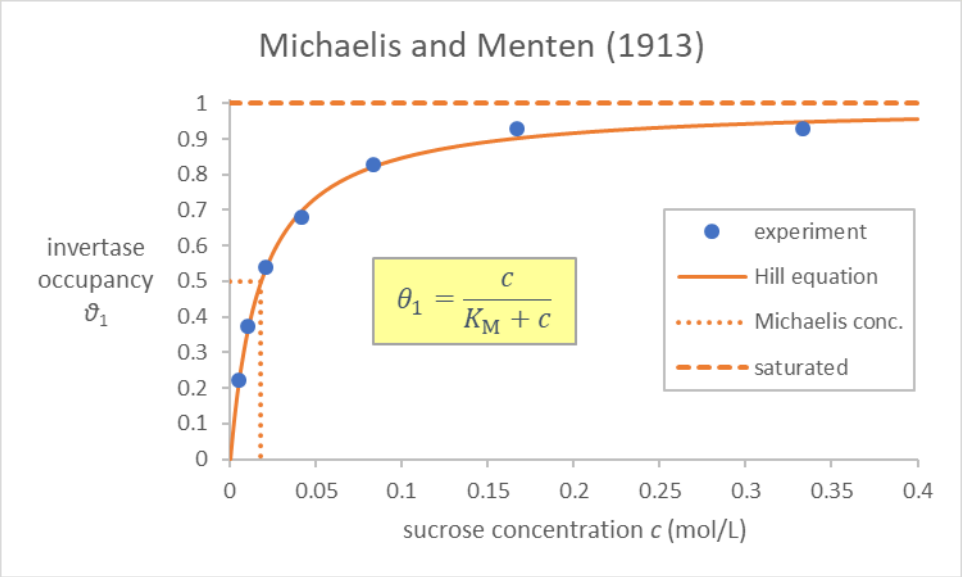

Fig.6.6 Excel chart showing century-old experimental confirmation that enzymes saturate. The graph shows data published by Michaelis and Menten in way back in 1913. You should have obtained the Michaelis constant ($K_M = 0.0179$ mol/L) and maximum velocity ($V_{max} = 3.91$ arb. units) by a non-linear least-squares fit to the data published by Michaelis and Menten. The experimental invertase enzyme occupancies were calculated using equation (6.22) and the theoretical prediction of saturation is given by the Hill-Langmuir equation (6.16). **Note:** This graph is not the answer to Q.6.36.

❑

Ch.9 Energy and the Boltzmann factor

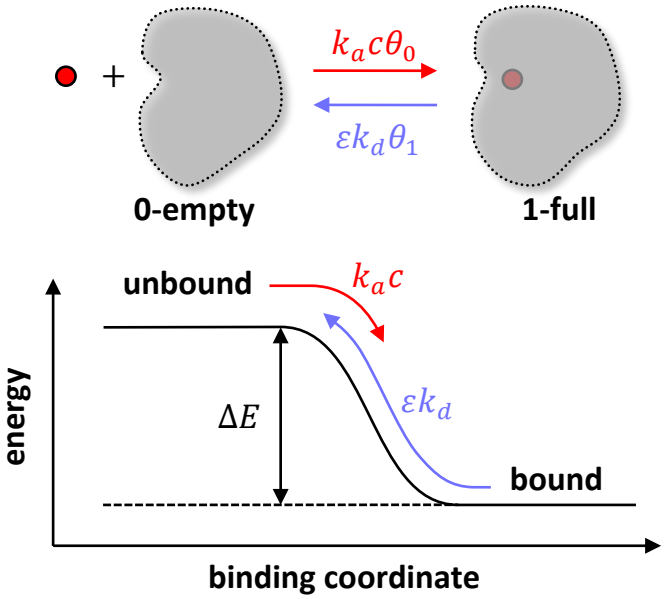

Fig.9.10 Schematic FD diagram of an O_2 molecule binding to myoglobin (upper) and energy diagram as a function of binding coordinate (lower). The energy difference $\Delta E \approx E_b$ is the binding energy, the energy required to remove a O_2 molecule from the Mb molecule's grasp.

$$\theta_1 = \frac{P_{O_2}}{B \exp\left(\frac{-\Delta H_{dis}}{RT}\right) + P_{O_2}} \tag{9.60}$$

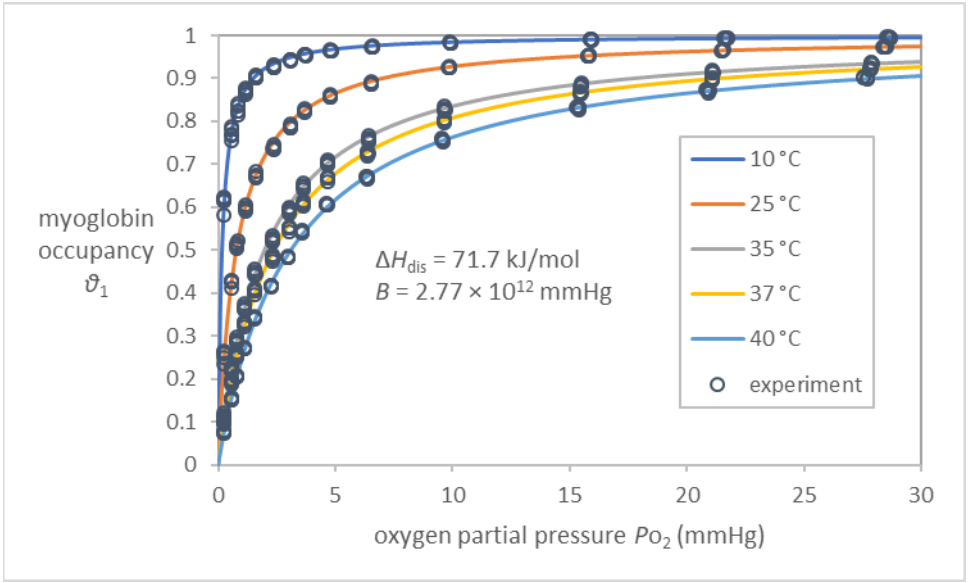

Fig.9.11 Excel chart comparing equation (9.60) of our model with experimental Mb-O_2 saturation data. Theoretical curves (solid lines) were fitted to equation (9.60) using nonlinear least-squares analysis (in Excel) resulting in $\Delta H_{dis} = 71.7$ kJ/mol and $B = 2.77 \times 10^{12}$ mmHg. Experimental data (symbols) reproduced (with permission) from Schenkman *et al.* [1997].

Ch.11 Membrane voltage and equivalent circuits

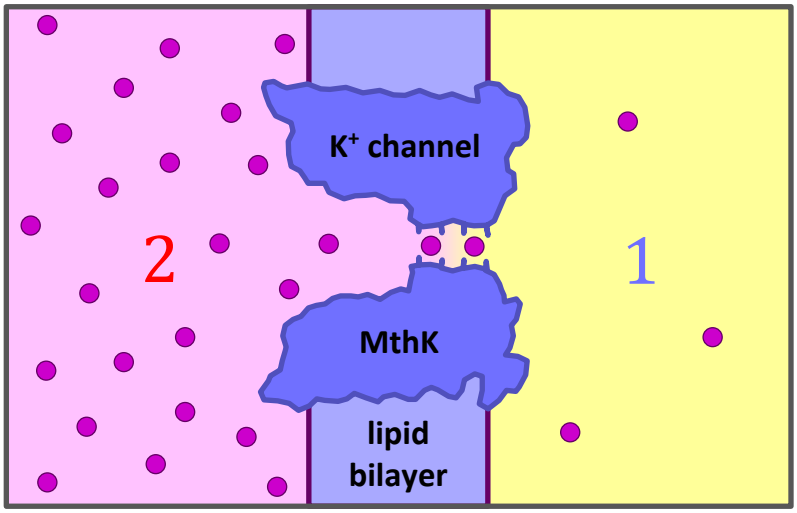

Fig.11.01 Schematic diagram of an open MthK potassium channel protein imbedded in a lipid bilayer membrane separating two solutions with differing K^+ ion concentrations (after Jiang *et al.* [2002]). The K^+ channel provides a single-file pathway (shown in cross-section) for potassium ions (circles) that makes the membrane semipermeable because only K^+ ions can pass through. **Note:** According to **the physiological convention**, box 2 (inside the cell) is on the left and box 1 (outside) is on the right.

Barrierless knock-on model

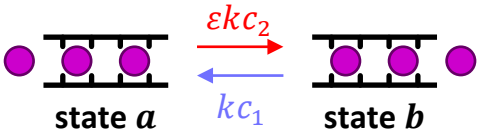

Fig.11.27 Hodgkin and Keynes knock-on mechanism. Permeation through the selectivity filter of an ion channel is modeled as a single *diffusive* jump. The energy factor in the outward direction from box 2 → 1 reflects the barrierless energy diagram Fig.11.06 (modified from Fig.11.02).

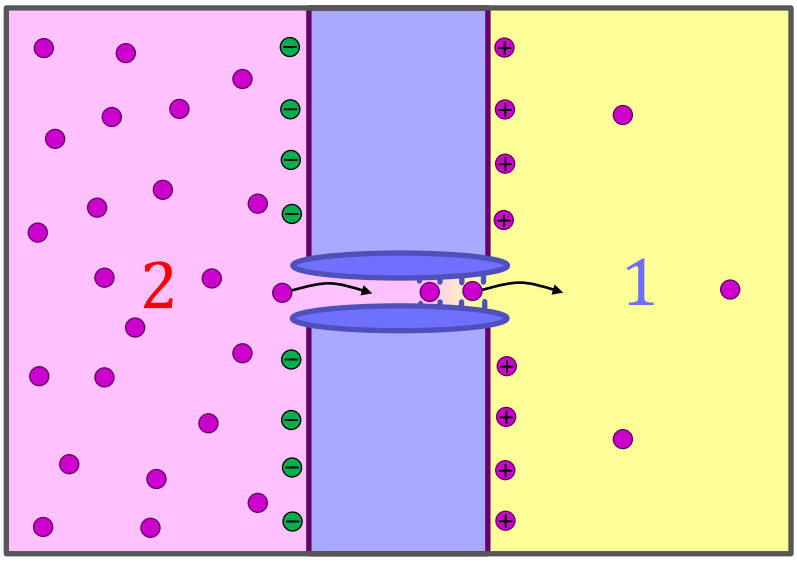

Fig.11.05 Schematic diagram of a cell membrane containing an open K^+ channel. K^+ ions have diffused from high to low concentration (box 2 → 1). The excess positive charges (shown as circles with a plus sign) have accumulated on the outside of the cell (box 1). They are attracted back towards their negative counter ions (shown as circles with a minus sign) that they left behind inside the cell. The charge separation produces a voltage difference ΔV because the attraction between the separated charges stores electric potential energy. I.e. the membrane acts like a **capacitor** (**SECTION 11.4**).

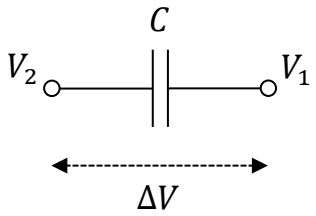

Fig.11.11 Equivalent circuit diagram of a cell membrane separating two solutions. The two open circles represent the inner (2) and outer (1) solutions that have a voltage difference $\Delta V = V_2 - V_1$. The **capacitor** (parallel lines symbol) has **capacitance** *C*.

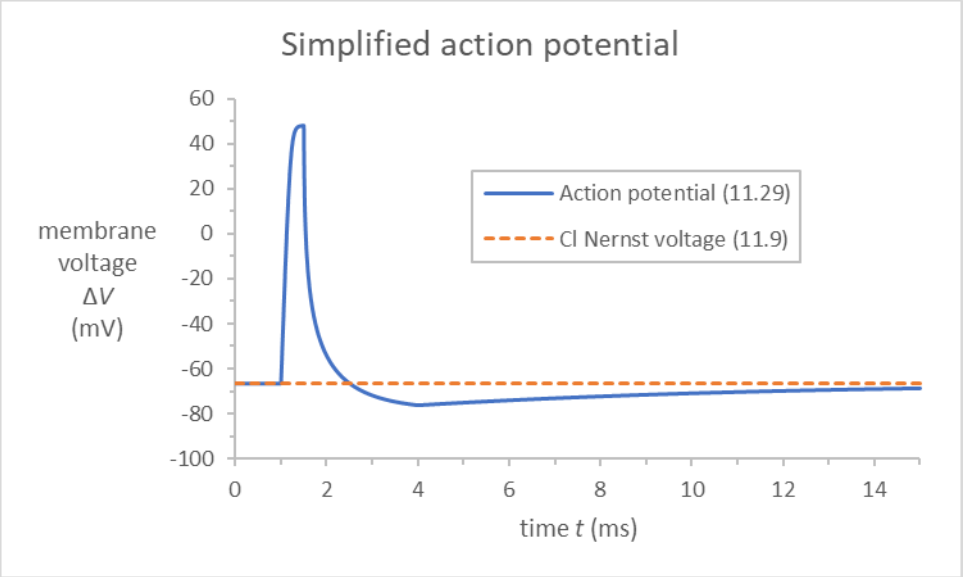

Fig.11.14 Excel chart showing a **simplified action potential** based on opening and closing Na^+ and K^+ channels "by hand" – see text. The graph begins with Cl^- channels open and the membrane voltage at about -70 mV, the Nernst voltage (11.9) for Cl^- ions, shown as a dashed line. The Cl^- channels always stay open throughout the graph. At time $t = 1$ ms, Na^+ channels open and the membrane voltage rapidly rises to about 50 mV. At time $t = 1.5$ ms, Na^+ channels close and K^+ channels open and the voltage drops down to about -80 mV. At time $t = 4$ ms, K^+ channels close leaving only the Cl^- channels open and the voltage slowly rises back to about -70 mV the Nernst voltage (11.9) for Cl^- ions.

Equivalent circuit for an ion channel in a membrane

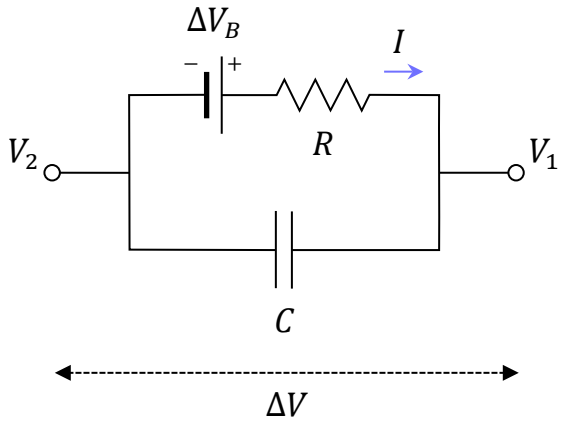

Fig.11.24 Equivalent circuit diagram of an open K^+ channel imbedded in a cell membrane separating two K^+ ion solutions with differing concentrations. The two open circles represent the inner (2) and outer (1) solutions in boxes 2 and 1 that have a voltage difference $\Delta V = V_2 - V_1$. The resistor has a voltage drop of $\Delta V_R = IR$ (11.63). The magnitude of the voltage across the battery is $\Delta V_B = -\Delta V_K$. The capacitor has a voltage difference of $\Delta V_C = \Delta V = IR - \Delta V_B$ (11.64). According to **the physiological convention**, positive current flows through the resistor R in the outward direction as indicated by the arrow labelled I.

Ch.12 COVID-19 and epidemiology

Summary manuscript arXiv:2104.08856

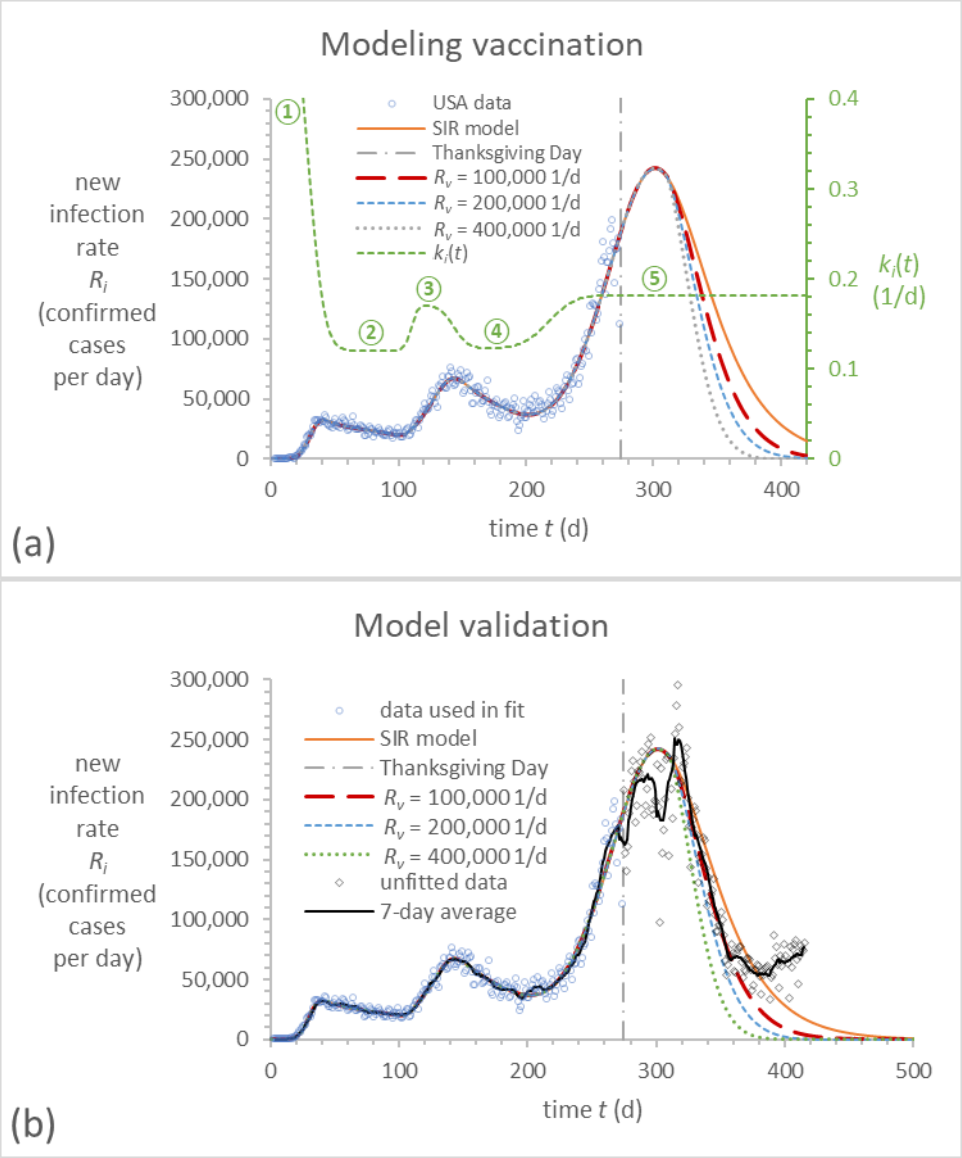

Fig. 12 Excel charts showing the predictions of the SIR-V model with vaccination (Fig. 11). The blue open circles show USA data reported as confirmed cases per day up to Thanksgiving Day (November 26, 2020). The solid orange line assumes no vaccinations and that the model population is 20% of the actual population (Fig. 10). The long-dashed, short-dashed, dotted, lines show the model predictions for an effective vaccination rate in the model population of $R_v = 100{,}000\ \mathrm{d}^{-1}$, $R_v = 200{,}000\ \mathrm{d}^{-1}$, and $R_v = 400{,}000\ \mathrm{d}^{-1}$, respectively. Chart **(a)** shows the infection rate coefficient $k_i(t)$ as a function of time on the secondary vertical axis. Circled numbers indicate the periods of the pandemic. Chart **(b)** shows USA data (grey diamonds) that were not used in the fit. The jagged thin black line shows the centered 7-day moving average of the reported USA data that validates the predictions of the SIR model with an effective vaccination rate of $R_v = 100{,}000\ \mathrm{d}^{-1}$ (data source OWID [14]).

Summary of the pedagogical approach

- Guided-inquiry self-study guides – ideal for online
  - flipped classroom – interactive HW in class time
- Active learning
  - student activities using preformatted spreadsheets
- Emphasis on skills
  - reading and interpreting graphs – semi-log graphs
  - fitting models to data – non-linear least-squares
- FD models of rate of change (→ calculus)
  - simple and realistic systems
- Thermodynamics from kinetics
- In a guided-inquiry environment, students discover that science is an evidence-based endeavor with testable hypotheses that are supported by experimental data.

For more information, free book chapters and other videos visit
http://circle4.com/biophysics

Supported by
NSF DUE 0836833

These materials are due to be published by Cambridge University Press

For free chapters, instructional videos and instructor guides visit http://circle4.com/biophysics/